International Journal of Bifurcation and Chaos, Vol. 5, No. 4 (1995) 1181–1192
© World Scientific Publishing Company

CONSTRUCTING INVARIANT MEASURES FROM DATA

GARY FROYLAND, KEVIN JUDD, ALISTAIR I. MEES and DAVID WATSON
Department of Mathematics, The University of Western Australia, Nedlands 6009, Western Australia

KENJI MURAO
Department of Electrical and Electronic Engineering, Miyazaki University, Miyazaki 889-21, Japan

Received June 21, 1994; Revised January 19, 1995

We present a method of approximating an invariant measure of a dynamical system from a finite set of experimental data. Our reconstruction technique automatically provides us with a partition of phase space, and we assign each set in the partition a certain weight. By refining the partition, we may make our approximation to an invariant measure of the reconstructed system as accurate as we wish. Our method provides us with both a singular and an absolutely continuous approximation, so that the most suitable representation may be chosen for a particular problem.

Int. J. Bifurcation Chaos 1995.05:1181-1192. Downloaded from www.worldscientific.com by THE UNIVERSITY OF NEW SOUTH WALES on 06/14/17. For personal use only.

1. Introduction

Let M be a finite-dimensional smooth compact manifold and $f\colon M \to M$ a C^2 map. The map f describes a discrete dynamical system on M. We assume that the orbits of f eventually lie near some limiting set $\Lambda \subset M$. Whether Λ is an attractor strictly contained in M, or is the whole of M, we do not care. A further assumption is that the system is transitive; this is to give some reason for hoping that almost all orbits have the same limiting distribution. We seek a single invariant measure for the system with support on Λ that describes the limiting distribution of Lebesgue almost all starting points. Such a measure, when it exists, (it is known to exist for Axiom A systems) is known as the Sinai–Bowen–Ruelle (SBR) measure. We of course do not know *a priori* whether such a measure exists for our map f. For the purposes of this paper we do not even know the function f itself; a reconstruction must be made from experimental data. What we are after is "the next best thing" to an SBR measure for our reconstructed map, whatever that may be.

We assume at the outset that we have been given a finite time series of data that has been successfully embedded in Euclidean space. This time series would have been a finite sequence of scalar values obtained from some readout function evaluated at various points in the state space of the dynamical system. The embedding theorem (Thm. 2.7 [Sauer *et al.*, 1991] for example) says that, under some assumptions on the underlying map, nearly every smooth readout function allows the time series to be embedded using the simple delay-coordinate technique. We do not concern ourselves with the technical matters of embedding; from now on we assume that the time series has been represented as an ordered sequence of points lying in $\mathbb{R}^d$, and proceed to reconstruct a map on $\mathbb{R}^d$ from this ordered sequence.

The convex hull of the embedded data points is triangulated using d-dimensional simplices. For

Int. J. Bifurcation Chaos 1995.05:1181-1192. Downloaded from www.worldscientific.com by THE UNIVERSITY OF NEW SOUTH WALES on 06/14/17. For personal use only.

arbitrary finite d, there are computer routines to do this [Watson, 1981, 1992]. Because the embedded points $\{y_1, \ldots, y_r\}$ are ordered so that $f(y_i) = y_{i+1}$, $1 \leq i \leq r-1$, there is a natural way to define a reconstruction of f [Mees, 1991]. In two dimensions, say, choose any simplex; it is fully described by its three vertices. The images of each of its vertices are known, and we *define* the image of the simplex under the reconstructed map to be simplex described by the images of the vertices. The reconstruction obtained from the triangulation approximates the map linearly on each simplex, producing a continuous, piecewise linear approximation, which we also denote by f (we never use the real f so there is no confusion). In this paper, we describe in detail a technique of approximating an invariant measure of f.

We give a brief outline of the process used, in order that the reader may have an overall picture in mind. The evolution of the deterministic dynamical system induced by the map f is approximated by a randomly perturbed system governed by a finite state Markov chain. The invariant density of the Markov chain will be used as an approximation of the invariant measure of f. We consider the centroid of each simplex as a state and define transition probabilities between them. These transition probabilities generate a transition matrix, which has an invariant density that assigns an asymptotic weight to each state. Our approximation of the invariant measure gives a weight to each of the centroids, equal to the weight of corresponding state. Because of the way that the transition probabilities are defined, it may be shown that as the diameters of the simplices go to zero, the invariant measures constructed from the invariant densities of the Markov chains approach an invariant measure of the triangulated map. We describe techniques of decomposing the simplices in the appropriate way to achieve such convergence. Our approach also offers the choice of either a singular or absolutely continuous approximation to the invariant measure, so that the best representation for a particular problem may be used.

2. A Method of Approximating Invariant Measures

2.1. *Representation of the deterministic system as a random system*

In order to obtain an approximation of the invariant measure of our deterministic system, we represent our deterministic system as a finite state Markov chain. The abstract states in the random system are to be identified with the centroids of the simplices of the triangulation, so that the evolution of our Markov chain is a random movement from centroids to centroids; see Fig. 1.

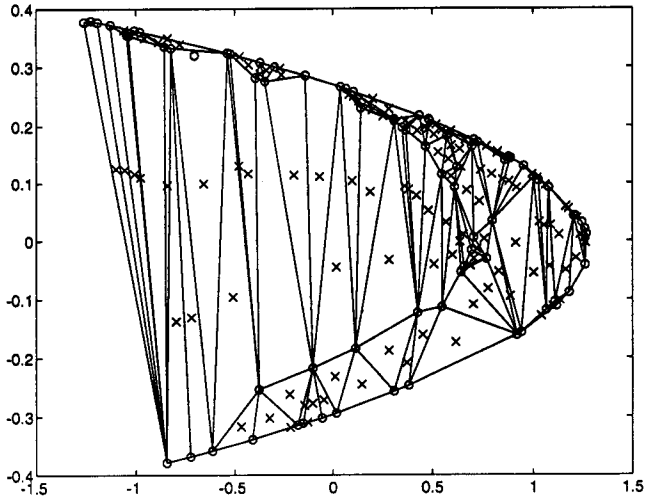

Fig. 1. Triangulation of an 80 point orbit of the Hénon map; data points are shown as circles. The states in the finite state Markov chain are to be identified with the centroids of the 120 triangles, shown by crosses.

By introducing randomness into the new representation, we compensate somewhat for the fact that our original system evolves on an infinite set, whereas our Markov chain moves between a finite set of points.

2.2. *Defining the approximation of the invariant measure*

Every finite state Markov chain has an invariant density, giving an asymptotic weight to each state. It is the invariant density of the Markov chain that we will be using as an approximation to the invariant measure of the deterministic system. The evolution of the Markov chain is governed by its *transition matrix*, which has all entries non-negative and row sums equal to one. We enumerate the simplices in some fashion, denoting the ith simplex by S_i, and putting x_i as the centroid of S_i. We then define the transition matrix P by

$$P_{ij} = \frac{\ell(945 f(S_i) \cap S_j)}{\ell(f(S_i))}, \quad 0 \leq i, j \leq \ell, \qquad (1)$$

where ℓ is Lebesgue measure on $\mathbb{R}^d$. P_{ij} is the probability that after one iteration of the Markov

chain, x_i moves to x_j. Note that $P_{ij} \geq 0$ and $\sum_{j=1}^{m} P_{ij} = 1$ (since the convex hull of the data points is mapped into itself), so that P is a stochastic matrix. Rather than having an initial point as in a deterministic system, we now have an initial distribution $\pi^{(0)} = \{\pi_1^{(0)}, \pi_2^{(0)}, \ldots, \pi_m^{(0)}\}$ for our Markov chain. Subsequent distributions are given by $\pi_j^{(n)} = \sum_{i=1}^{m} \pi_i^{(n-1)} P_{ij}$, with $\pi^{(n)} = \pi^{(0)} P^n$. The invariant density π of the finite state Markov chain satisfies $\pi = \pi P$. Throughout, we assume that our Markov chains are ergodic so that they have a unique invariant density.

2.3. *Increasing the accuracy of the approximation*

We define

$$\varepsilon = \max_{1 \leq i \leq m} \frac{\text{diam}(S_i)}{2},$$

the maximal radius of all the simplices in the triangulation, and set

$$\omega_f(\varepsilon) = \sup_{\substack{x,y \in M \\ \|x-y\| < \varepsilon}} \|f(x) - f(y)\|,$$

the modulus of continuity of f. Here $\text{diam}(S_i)$ is twice the maximum distance between the centroid x_i and each of the vertices of S_i. The definition of P_{ij} makes our Markov chain a *small random perturbation* [Kifer, 1988] of the deterministic map f. This means that if we are at the centroid x_i, and $P_{ij} > 0$, then $f(x_i)$ is not too far from x_j. An upper bound on the distance between $f(x_i)$ and x_j is given by $\text{diam}(f(S_i))/2 + \text{diam}(S_j)/2 < \omega_f(\varepsilon) + \varepsilon$. This is because the triangulated map is linear on simplices and $f(x_i)$ is the centroid of $f(S_i)$. So under the evolution of our Markov chain, the centroid x_i may move to any of the centroids x_j contained in the balls centred at $f(x_i)$ with radii $\text{diam}(f(S_i))/2 + \text{diam}(S_j)/2$; see Fig. 2. One may think of our Markov chain as a randomly perturbed system in the following way. Starting at the centroid x_i in our discrete set, the true image $f(x_i)$ is computed, then randomly perturbed by an amount less than $\omega_f(\varepsilon) + \varepsilon$ to a nearby centroid contained in our finite set.

By refining our triangulation, that is, decreasing the maximal size of our simplices, we are able to reduce the perturbations acting on f, and the evolution of the random system will become increasingly similar to that of the deterministic system.

Consider a sequence of triangulations, with maximal radii $\varepsilon_1 > \varepsilon_2 > \cdots > \varepsilon_n > \cdots$, such that

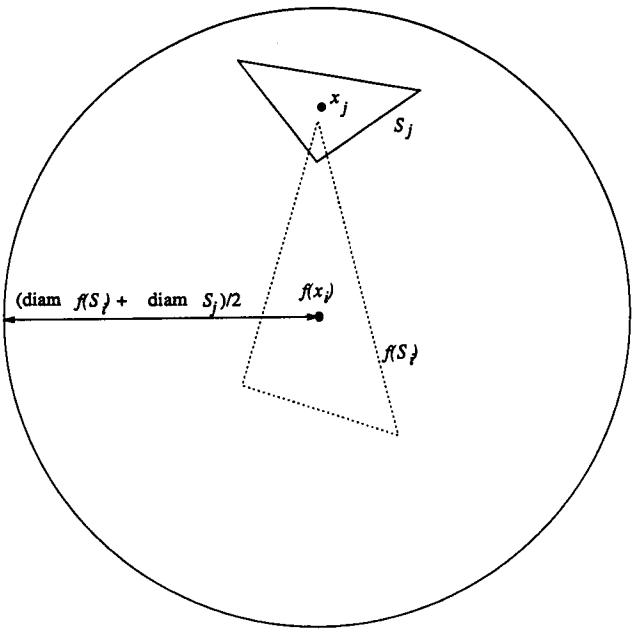

Fig. 2. Intersection of $f(S_i)$ and S_j bounds the distance between $f(x_i)$ and x_j. Thus x_i may move to any of the centroids x_j contained in the balls centred at $f(x_i)$ with radii $\text{diam}(f(S_i))/2 + \text{diam}(S_j)/2$. One may think of the evolution of the Markov chain as computing the true image of a centroid and then perturbing the result a small amount to some randomly chosen centroid.

$\lim_{n \to \infty} \varepsilon_n = 0$. Denote the corresponding transition matrices and invariant densities by P^{ε_n} and π^{ε_n}, respectively. By identifying the density π^{ε_n} with the measure $\sum_{i=1}^{m_n} \pi_i^{\varepsilon_n} \delta_{x_i}$, ($\delta_{x_i}$ is the delta measure with support x_i), we may consider π^{ε_n} as an element of $\mathcal{M}(M)$, the space of all (Borel) probability measures on M. Since M is compact, so is $\mathcal{M}(M)$ and we may extract a limit point $\tilde{\pi}$ from the sequence $\{\pi^{\varepsilon_n}\}_{n=1}^{\infty}$. It is easy to show [Khas'minskii, 1963] that $\tilde{\pi}$ is in fact an invariant measure of the map f. However, at this stage, it is difficult to say anything else.

2.4. *Difficulties with estimating invariant measures of dynamical systems*

Deterministic dynamical systems have many invariant measures; semi-colon for example, the measure formed from equally weighted delta measures with support any periodic orbit. We would really like to have an estimate of the "physical" or "natural" measure of the dynamical system which gives areas of high density proportionally more weight than areas of low density. Experimentalists usually take

Int. J. Bifurcation Chaos 1995.05:1181-1192. Downloaded from www.worldscientific.com by THE UNIVERSITY OF NEW SOUTH WALES on 06/14/17. For personal use only.

the physical measure to be the limiting distribution of points of long orbits which show up on a computer for most initial points. This description is far from satisfactory for a number of reasons. Firstly, the computer can only store a finite number of states, so that the computed orbit is eventually periodic; such behaviour may not displayed by the real system. Secondly, the computed orbit is subjected to round-off errors at each iteration, so that there is no guarantee that the eventually periodic orbit is anything like a real orbit of the system. Both of these problems are machine dependent, varying from computer to computer. The difficulties do not stop here, however. Ignoring the imprecision of computers, there is still very little known about the characterisation or existence of "physical" invariant measures of general dynamical systems. Only in relatively simple systems, such as expanding or unimodal maps in one dimension and Axiom A systems in higher dimensions, do notions of "physical" measures take on precise mathematical meanings. Sadly, we do not provide any solutions to these problems here; they are merely mentioned to make the reader aware of some of the difficulties one faces when estimating invariant measures.

We argue that the invariant measures we obtain have physical significance as they arise as limits of invariant measures of systems subjected to small amounts of noise.

3. How to Decompose the Simplices

The size of the perturbations are governed by the radii of the triangles, not the volumes, so that any simplex decomposition technique must be radii reducing. In two dimensions, one may split a triangle up into four identical triangles, each similar to the original, with half its diameter; see Fig. 3.

The vertices of the smaller triangles will consist of the original vertices as well as the midpoints of the sides of the original triangle. Since the images of all the points in the original triangle are known, the images of the smaller triangles are easily computed. In three dimensions, the decomposition problem is not as straightforward, as there is no regular splitting of a tetrahedron. By placing similar tetrahedrons of half-diameter at each of the four corners of the original tetrahedron, one is left with an octahedron in the middle. The octahedron may then be decomposed into four more tetrahedra. The splitting methods we use are ones which reduce

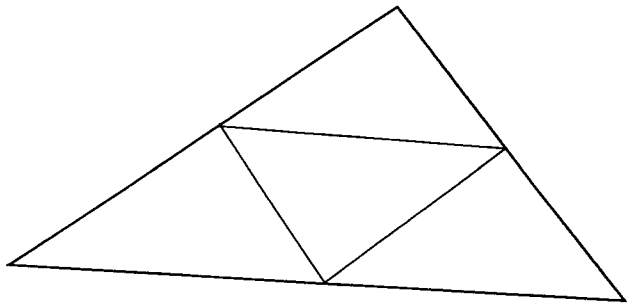

Fig. 3. Decomposition of simplices in two dimensions. Each of the smaller triangles has a diameter half that of the original.

the diameter of the simplex while not producing too many subsimplices. In any dimension there is a natural way of splitting simplices called barycentric subdivision. However, this subdivision reduces the diameter too slowly and produces too many subsimplices. For example, in two dimensions, six subsimplices are created for a diameter reduction of two-thirds its original; our method produces four subsimplices for a diameter reduction of one half. In three dimensions, barycentric subdivision would produce 24 subsimplices for a diameter reduction of only three quarters. The situation worsens in higher dimensions; in general, barycentric subdivision produces $(d+1)!$ subsimplices for a diameter reduction of $d/(d+1)$ in dimension d.

In order to decrease the maximum perturbation, simplices whose image is large or are themselves large should be targeted for splitting up. Because of the typically large variation in simplex diameter, splitting up the larger simplices first is more efficient than blindly splitting up all the simplices the same number of times. Some simplices may initially need to be split repeatedly in order to reduce their diameter to a level comparable to most simplices in the triangulation. We may make the simplices as small as we desire (subject to computer time and memory constraints), thus reducing the perturbations, and increasing the accuracy of our estimate of the invariant measure.

4. Represention of the Approximation

Recall that our approximation of the invariant measure is a finite convex combination of delta measures, with each delta measure having support at the centroid of some simplex in the triangulation; see Fig. 4(a). To integrate a function $g\colon M \to \mathbb{R}$ with respect to this representation, one merely sums

Int. J. Bifurcation Chaos 1995.05:1181-1192. Downloaded from www.worldscientific.com by THE UNIVERSITY OF NEW SOUTH WALES on 06/14/17. For personal use only.

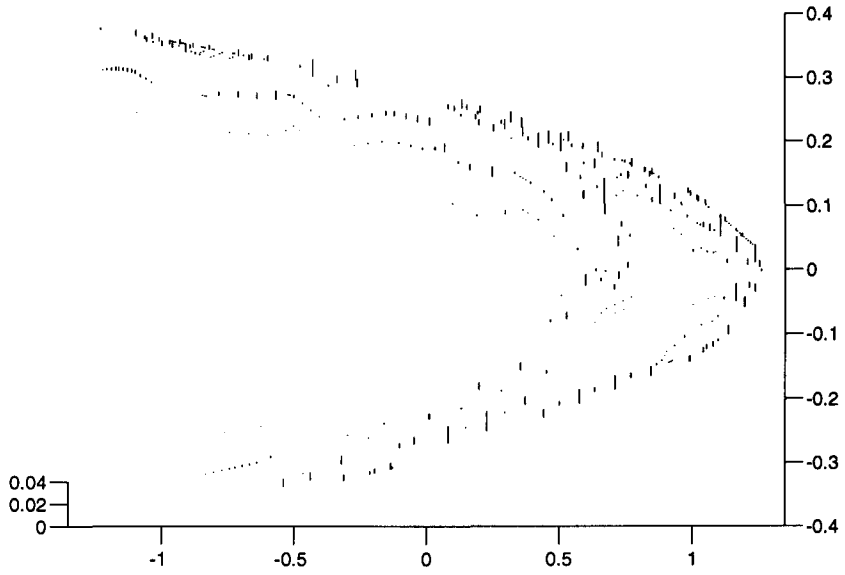

(a)

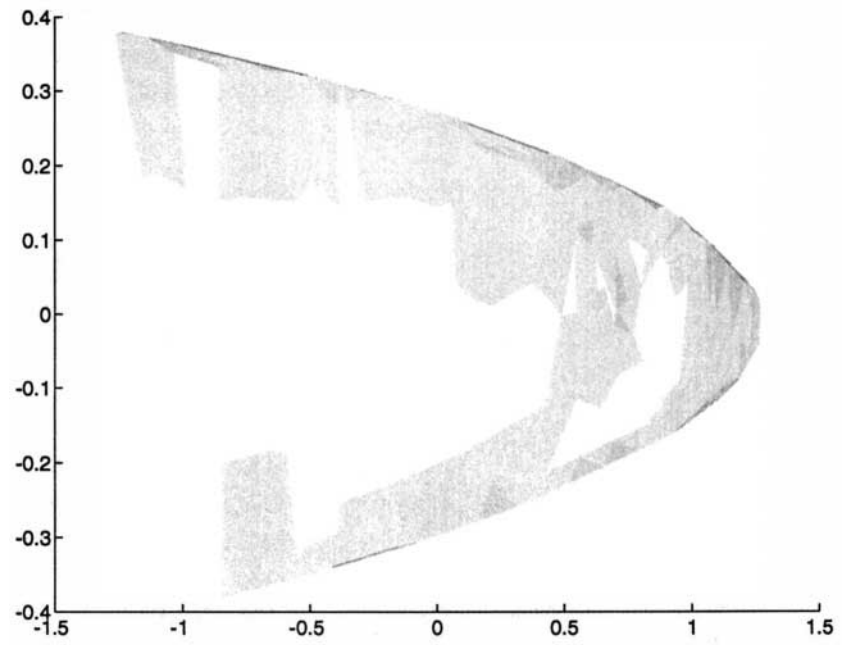

(b)

Fig. 4. (a) Singular approximation of an invariant measure of the Hénon map using an 80 point orbit. The measure is a convex combination of 366 delta measures, which are shown as spikes in this two-dimensional plot. The base of the spike represents the position of the support of the measure and the height represents the relative weight given to the centroid. (b) Absolutely continuous approximation of the invariant measure of the Hénon map using an 80 point orbit and 366 triangles. Darker shades of grey represent regions of higher density.

the values of g evaluated at the centroids and weights them according to the invariant density π, so that $\int_M g\, d\pi = \sum_{i=1}^{m} g(x_i)\pi_i$. This approximation is singular with respect to Lebesgue measure, that is, the measure gives sets of Lebesgue measure zero (namely, the centroids) positive measure. There may be circumstances in which an absolutely continuous estimate of an invariant

Int. J. Bifurcation Chaos 1995.05:1181-1192. Downloaded from www.worldscientific.com
by THE UNIVERSITY OF NEW SOUTH WALES on 06/14/17. For personal use only.

measure is required, that is, a measure which assigns sets of Lebesgue measure zero, zero measure. For example, Perron–Frobenius theory may only be applied to absolutely continuous measures. Such an estimate may be constructed from the singular approximation by uniformly distributing the weight concentrated at the centroids over their respective simplices; see Fig. 4(b). We define the absolutely continuous representation π_{abs} by

$$\pi_{\text{abs}}(A) = \sum_{i=1}^{m} \frac{\ell(A \cap S_i)}{\ell(S_i)} \cdot \pi_i \,, \tag{2}$$

for A a Borel measurable set, so that

$$\int_M g(x) d\pi_{\text{abs}}(x) = \sum_{i=1}^{m} \frac{\pi_i}{\ell(S_i)} \int_{S_i} g(x)\, d\ell(x) \,. \tag{3}$$

The absolutely continuous representation is equivalent to the singular representation in the following sense. If $\{\pi^{\epsilon_n}\}_{n=1}^{\infty}$ is a sequence of (singular) probability measures converging weakly to an invariant measure $\tilde{\pi}$, then the sequence of absolutely continuous probability measures $\{\pi^{\epsilon_n}_{\text{abs}}\}_{n=1}^{\infty}$ constructed from the π^{ϵ_n} as above also converges to $\tilde{\pi}$. In particular, this shows that weak limits of the absolutely continuous measures are invariant.

5. Examples

For ease of presentation, we restrict our examples to the two-dimensional case, and estimate invariant measures of the Hénon map f_1: $X \to X$, $X \subset \mathbb{R}^2$ and a nonlinear torus map f_2: $S^1 \times S^1 \to S^1 \times S^1$.

$$f_1(x, y) = (-1.4x^2 + y + 1,\, 0.3x) \,. \tag{4}$$

$$f_2(x, y) = (y + 0.1\sin(2\pi x) + 2x + 0.2\cos(2\pi x),\; x + 0.1\cos(2\pi x)) \pmod 1 \,. \tag{5}$$

We give three examples, two for the Hénon map and one for the torus map. The first example is an estimation of the invariant measure of the Hénon map from an 80 point orbit. The triangles and centroids of the nontransient states of the induced Markov chain are shown in Fig. 1. To decrease the radii of the triangles, each of the triangles was split up twice, so that the resulting maximal triangle diameter was a quarter of its original value. After computing the transition matrix, it is easy to see that some states may be neglected immediately. If the transition matrix has a column of zeros, that is, $P_{ij} = 0$ for all $i = 1, \ldots, m$ for some j, then state j may be thrown away. This is because a column of zeros in the jth position means that all image simplices have empty intersection with S_j; that is, nothing is mapped into S_j. After throwing away such states, there are still other states which do have pieces of simplices mapped into them, but the intersections are so small that their asymptotic density is zero. These states are called transient and have zero weight; we are concerned only with the nontransient states as they are the ones that contribute to the approximation of the invariant measure. In this example, the original triangulation had 124 triangles, four of which corresponded to zero column sums of the transition matrix. These four were neglected, and the remaining 120 split up twice, discarding simplices not intersecting the image triangulation after the first splitting. This produced 628 triangles, 437 of which intersected the image triangulation, 366 of these being nontransient. Both the singular and absolutely continuous representations of the estimates of an invariant measure of the reconstruction obtained from the 80 point orbit are shown in Fig. 4.

Our second example is an illustration of what effect smaller perturbations have on the estimates of the invariant measures. Here, we use 87 data points, chosen so that the triangles are smaller than

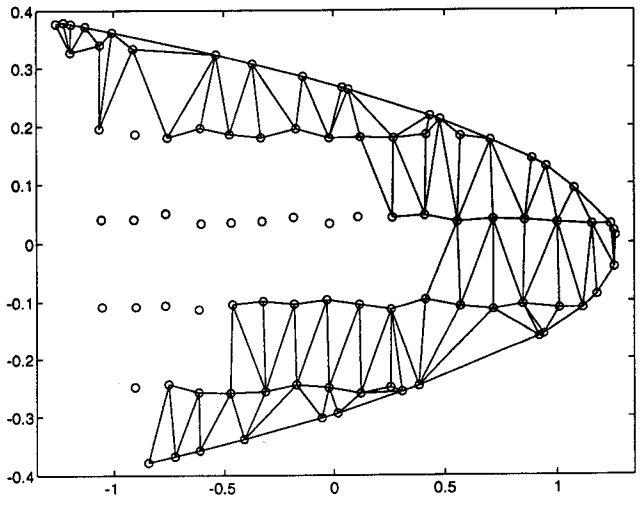

Fig. 5. Nontransient triangles of the triangulation obtained from 87 data points generated by the Hénon map. The original triangulation contained 139 triangles, but only 86 of these intersected the image triangulation, so that the 53 triangles could be removed without any splitting up required. All of the remaining 86 triangles were nontransient.

Int. J. Bifurcation Chaos 1995.05:1181-1192. Downloaded from www.worldscientific.com by THE UNIVERSITY OF NEW SOUTH WALES on 06/14/17. For personal use only.

those arising from a typical orbit of 87 points. The nontransient triangles are shown in Fig. 5.

We are able to remove 53 triangles straight away without any splitting. The Hénon attractor has a large gap between the two "arms" on the left hand side, so that triangulations arising from a time series always produce large triangles spanning this gap. It should be noted, however, that these triangles

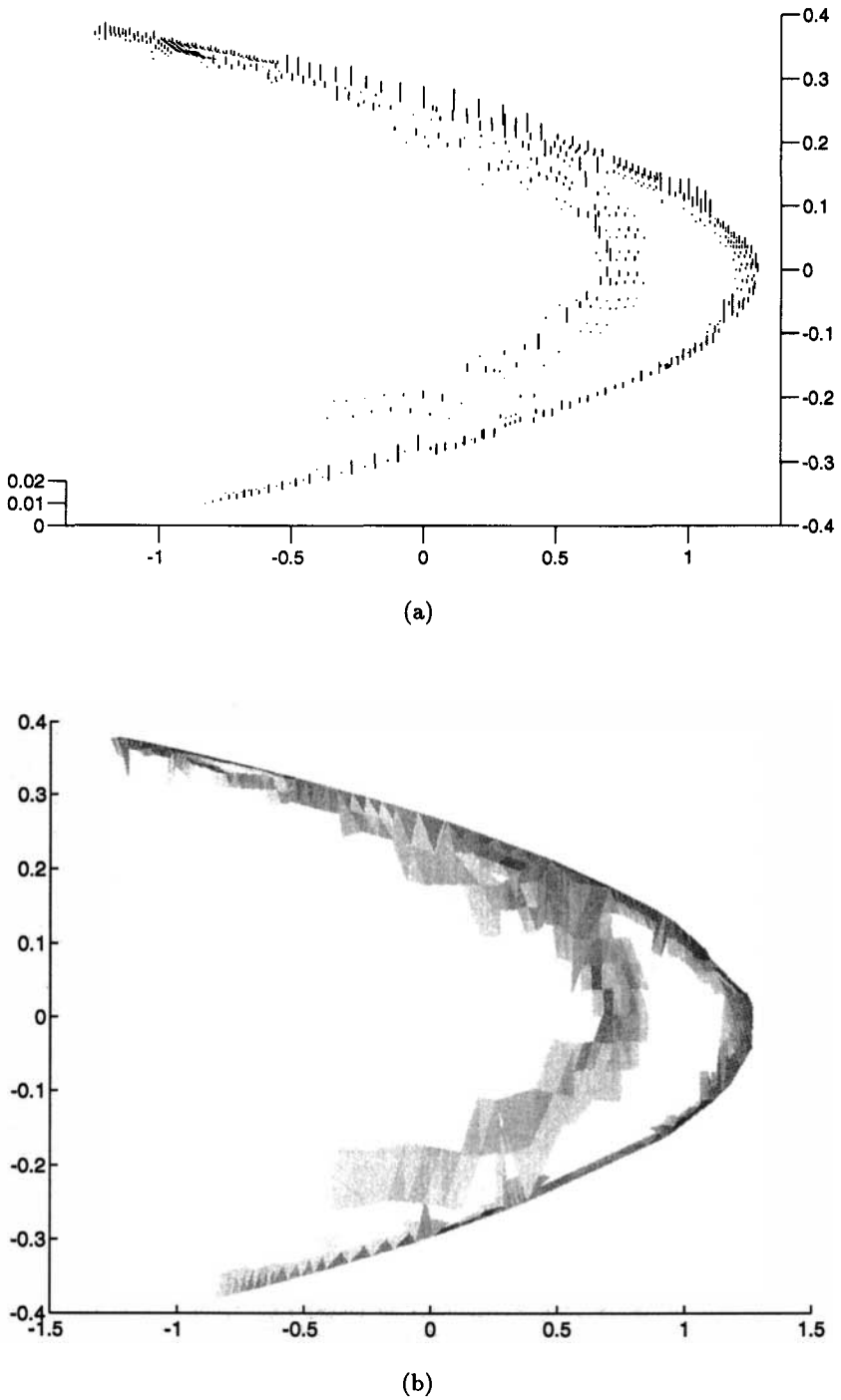

Fig. 6. (a) Singular approximation of the invariant measure of the Hénon map using 87 data points. The measure is a convex combination of 708 delta measures, which are shown as spikes in this two-dimensional plot. The base of the spike represents the position of the support of the measure and the height represents the relative weight given to the centroid. (b) Absolutely continuous approximation of the invariant measure of the Hénon map using 87 data points and 708 triangles. Darker shades of grey represent regions of higher density.

Int. J. Bifurcation Chaos 1995.05:1181-1192. Downloaded from www.worldscientific.com
by THE UNIVERSITY OF NEW SOUTH WALES on 06/14/17. For personal use only.

Table 1. Perturbation Values of the Sequence of Splittings of the two Triangulations of the Hénon Map.

Number of Data Points	Number of NonTransient States	Maximum Perturbation	Mean Perturbation
80	120	0.4728	0.0853
80	366	0.2025	0.0386
87	86	0.4169	0.0866
87	314	0.1647	0.0349
87	708	0.0990	0.0191

Int. J. Bifurcation Chaos 1995.05:1181-1192. Downloaded from www.worldscientific.com by THE UNIVERSITY OF NEW SOUTH WALES on 06/14/17. For personal use only.

are not as large as they appear, because of the difference in the scaling of the two coordinates. The action of the map is also such that triangles that are mapped onto one of the "arms" are stretched into long, thin triangles with large diameter. By choosing points which are more equally spaced throughout the convex hull of the data points, these problems are avoided. Of course, we can split up the triangles generated by a time series so that they are as small as we please; it just takes time. Starting with specially chosen data points speeds things up.

We applied the splitting procedure twice, preferentially targeting larger triangles and triangles with large images. The first splitting produced 482 triangles, 339 of which intersected the image, with 314 of these being nontransient. The 339 triangles were again split up to obtain 1047 simplices, with 764 intersecting the image triangulation and 708 nontransient. Both representations of the estimates of the measures are shown in Figs. 6(a) and 6(b).

In order to quantify the "average" perturbation that the random system is subjected to, we define a mean perturbation by

$$\text{MeanPerturbation} = \sum_{i=1}^{m} \pi_i \sum_{j=1}^{m} P_{ij} d_{ij} ,$$

where d_{ij} is the distance between the centroids of $f(S_i)$ and S_j. The values of the maximum and mean perturbation for both reconstructions of the Hénon map are shown in Table 1.

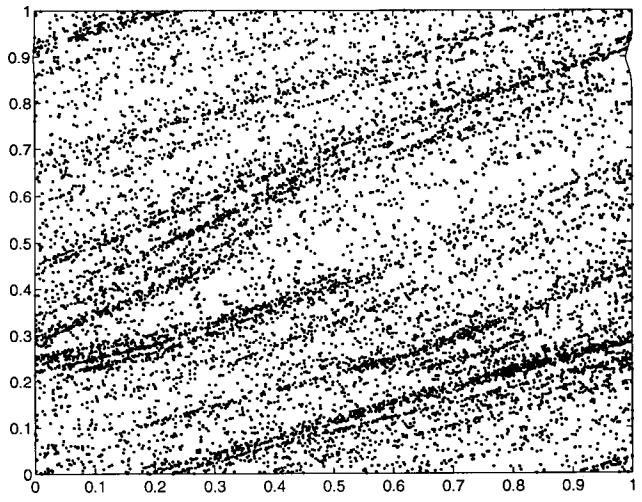

Fig. 7. Orbit of length 10 000 generated by the piecewise linear approximation to (5) using an orbit of length 11. The piecewise linear approximation is a good one in the sense that long orbits generated by the true map have similar distributions. Here the torus has been unwrapped onto the unit square.

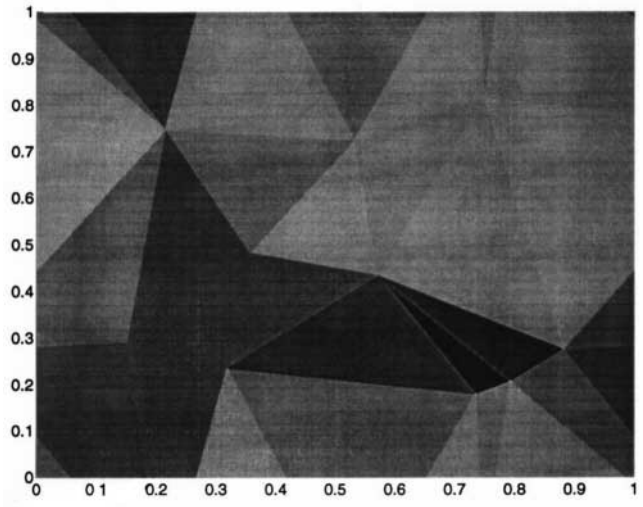

Fig. 8. Absolutely continuous approximation of the invariant measure of (5) using an 11 point orbit and a partition of 20 triangles. Darker shades of grey represent regions of higher density. The torus has been unwrapped onto the unit square.

Int. J. Bifurcation Chaos 1995.05:1181-1192. Downloaded from www.worldscientific.com
by THE UNIVERSITY OF NEW SOUTH WALES on 06/14/17. For personal use only.

[Kohda & Shinji, 1992] have estimated an invariant measure of the Hénon map using a related method. They approximate the infinite dimensional Perron–Frobenius operator by a finite dimensional operator, and compute the fixed point of this simpler operator. Fixed points of the Perron–Frobenius operator correspond to absolutely continuous invariant measures, and they argue that the density obtained from their finite dimensional approximation is close to an important invariant measure of the Hénon system.

Our third example estimates the invariant measure of the nonlinear torus map (5). We use an 11 point orbit to reconstruct the piecewise linear approximation, with the resulting triangulation containing 20 simplices. For calculation and pictorial representation of the invariant density, we unwrap the torus onto the unit square, identifying opposing edges and giving them the same orientation. An orbit of length 10 000 generated by the piecewise linear map is shown in Fig. 7; an almost identical distribution appears for long orbits generated by the true map. Figure 8 is the absolutely continuous approximation of the invariant density, using the original 20 triangles. The 10 000 point orbit was then used to compute a histogram on the 20 set partition, the result is shown in Fig. 9.

Comparing Figs. 8 and 9 we see that even with large perturbations the approximation on this coarse partition is not too bad. The partition was refined by splitting up the triangles as before to reduce the maximal diameter. The splitting produced 200 triangles, all of which are nontransient. The corresponding pictures to Figs. 8 and 9 are shown in Figs. 10 and 11.

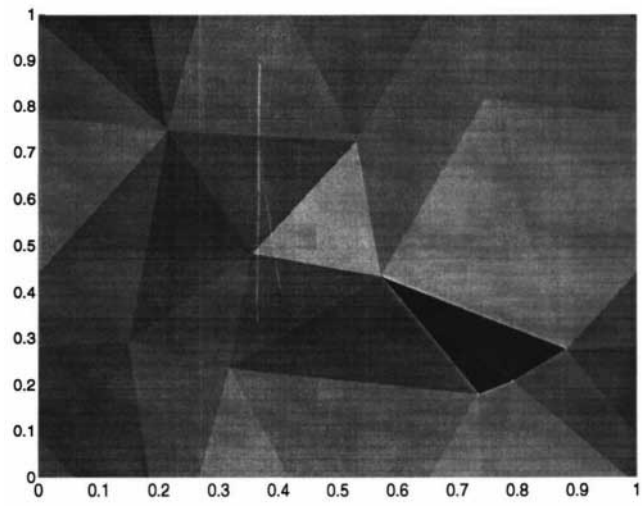

Fig. 9. Histogram generated by the 10 000 point orbit in Fig. 7 using the 20 set partition shown in Fig. 8. Darker shades of grey represent regions of higher density. The torus has been unwrapped onto the unit square here.

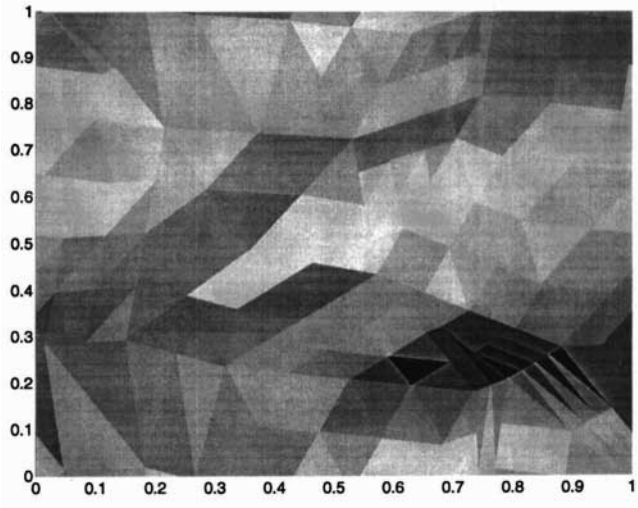

Fig. 10. Absolutely continuous approximation of the invariant measure of (5) using an 11 point orbit and a partition of 200 triangles. Darker shades of grey represent regions of higher density. The torus has been unwrapped onto the unit square.

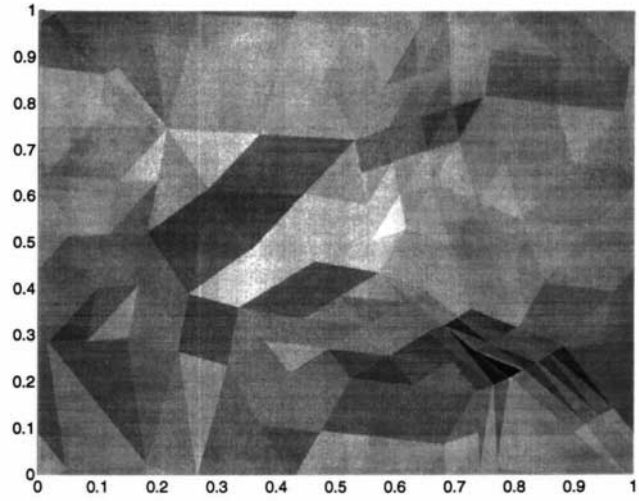

Fig. 11. Histogram generated by the 10 000 point orbit in Fig. 7 using the 200 set partition shown in Fig. 10. Darker shades of grey represent regions of higher density. The torus has been unwrapped onto the unit square here.

Again we see that the densities shown in Figs. 10 and 11 are not very different, suggesting that the approximation shown in Fig. 10 is reasonable. One should keep in mind that this approximation has been generated by an orbit of only eleven points.

Table 2. Perturbation Values of the Original and Split Triangulations of the Nonlinear Torus Map.

Number of Data Points	Number of NonTransient States	Maximum Perturbation	Mean Perturbation
11	20	0.4932	0.1753
11	200	0.2456	0.0621

Table 2 shows the perturbation values for the original and split triangulations.

Similar work has been done [Mees *et al.* 1993], where the invariant density of (5) is estimated from 11 and 101 point orbits using the technique of Kodha & Shinji [1992]. The method used to find the forward image of the triangulation on the torus is detailed in Mees *et al.* [1993].

5.1. *"Pushing forward" the approximation*

As a possible way of increasing the accuracy of the approximations, one could map the approximate measure forward one iteration. For example, in the case of the singular approximation, we take the spike with base x_i and reposition it at $f(x_i)$. In the case of the absolutely continuous approximation, (which is derived from a corresponding singular approximation), the weight is spread uniformly over $f(S_i)$, after repositioning the spike as above. All of this amounts to a mapping $\tilde{f}$: $\mathcal{M}(M) \to \mathcal{M}(M)$ from the space of probability measures to itself, given by $\tilde{f}(\pi) = \pi \circ f^{-1}$. By definition, the *exact* invariant measure will be a fixed point of $\tilde{f}$, so that one may think that good approximations of the exact invariant measure will not change a great deal under $\tilde{f}$. Because the dynamical system typically has an attractor, it is reasonable to suppose that mapping the measure forward will increase the accuracy of the support of the measure, because it will be attracted towards the attractor. This argument has been made rigorous (Kifer [1988], p. 143) for uniformly hyperbolic attractors using

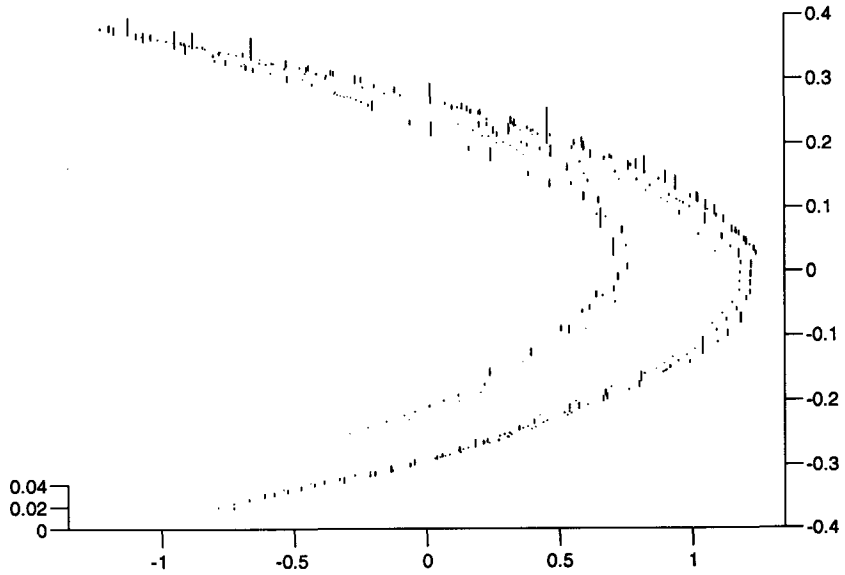

Fig. 12. Singular approximation of the invariant measure of the Hénon map using an 80 point orbit. The measure is a convex combination of 366 delta measures, which are shown as spikes in this two-dimensional plot. This measure is constructed by placing the weight given to the centroid x_i at the position $f(x_i)$. In other words, if π is the measure shown in Fig. 4(a), then this measure denoted $\hat{\pi}$ equals $\pi \circ f^{-1}$. The base of the spike represents the position of the support of the measure and the height represents the relative weight given to the centroid.

Int. J. Bifurcation Chaos 1995.05:1181-1192. Downloaded from www.worldscientific.com by THE UNIVERSITY OF NEW SOUTH WALES on 06/14/17. For personal use only.

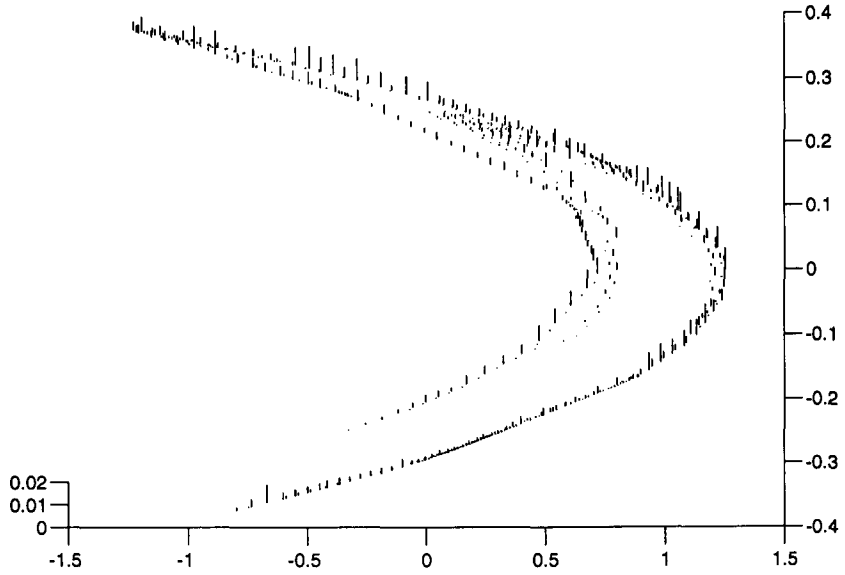

Fig. 13. Singular approximation of the invariant measure of the Hénon map using 87 data points. The measure is a convex combination of 708 delta measures, which are shown as spikes in this two-dimensional plot. This measure is constructed by placing the weight given to the centroid x_i at the position $f(x_i)$. In other words, if π is the measure shown in Fig. 6(a), then this measure denoted $\hat{\pi}$ equals $\pi \circ f^{-1}$. The base of the spike represents the position of the support of the measure and the height represents the relative weight given to the centroid.

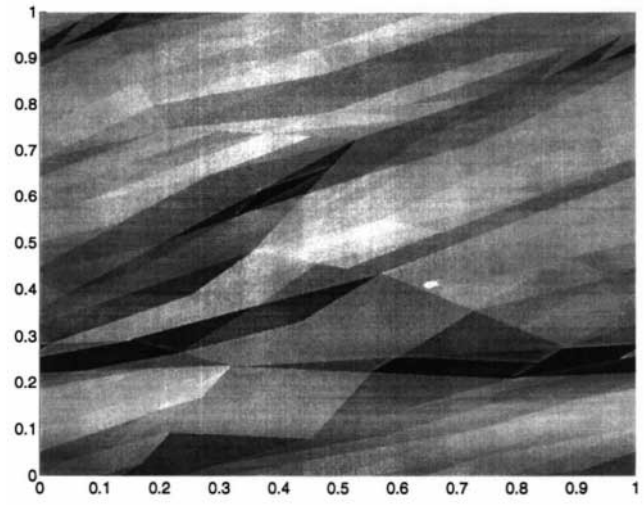

Fig. 14. Absolutely continuous approximation of the invariant measure of the nonlinear torus map (5) using an 11 point orbit. Darker shades of grey represent areas of higher density. This measure is constructed by placing the weight given to the centroid x_i at the position $f(x_i)$, and then distributing this weight uniformly throughout $f(S_i)$. In other words, if π is the measure shown in Fig. 10, then this measure denoted $\hat{\pi}$ equals $\pi \circ f^{-1}$. Here, the torus has been unwrapped onto the unit square.

shadowing properties. For Axiom A attractors, it is known that the (unique) limit point of repeated push-forwards of any absolutely continuous measure with support contained in the basin of attraction is the SBR measure [Ruelle, 1976]. So roughly speaking, pushing forward our absolutely continuous approximation enough, should improve its accuracy. To satisfy the reader's curiosity, Figs. 12–14 show the results of mapping forward the approximations to the invariant densities of our three examples. As far as the accuracy of the support goes, Figs. 12 and 13 show marked improvements. Comparing Fig. 14 with Fig. 7 shows we do quite well with one push-forward.

6. Discussion

We have described a method of approximating an invariant measure of a reconstruction of a dynamical system from a finite set of data. The approximation may be made as accurate as desired, subject to computing accuracy, time, and memory. Although we have only considered estimating an invariant measure of the reconstructed system, we can do better than this if we have more data points at our disposal. If the diameter of the triangles goes to zero, by virtue of there being more data points made available, rather than splitting them up, the limiting measure is an invariant measure of the *true* system. This is because the accuracy of the reconstruction also depends on the diameter of

Int. J. Bifurcation Chaos 1995.05:1181-1192. Downloaded from www.worldscientific.com
by THE UNIVERSITY OF NEW SOUTH WALES on 06/14/17. For personal use only.

the triangles. Splitting the triangles increases the accuracy of the Markov chain representation, but adds no new information to the reconstruction. To expect a better approximation of an invariant measure of the *true* map, one requires more information in the form of more data points.

We are still left with the problem that we don't know which invariant measure we are approximating. One would hope that it is an interesting or important invariant measure of the system; see discussion in Diamond *et al.* for possible candidates. As mentioned earlier, little is known about invariant measures of general dynamical systems. Kifer [1988, p. 157] has shown that for perturbations based on continuous diffusions with exponential decay, the limiting measure is the Sinai–Bowen–Ruelle (SBR) measure in the case of Axiom A attractors. Young [1986] has shown a similar result for continuous linear diffusions restricted to ε-balls. For Axiom A attractors, the SBR measure has its support contained in the attractor, is absolutely continuous in unstable directions, and is the limiting distribution for all orbits starting in a set of full Lebesgue measure. It is generally considered to be the "physical" measure for hyperbolic systems.

Our perturbations do not fall into the class considered in Kifer [1988], though it is hoped that a similar result is true for the limiting measures we obtain. A partial result [Froyland] is that in the case of two-dimensional Anosov systems, our construction yields the SBR measure in the zero noise limit, provided our partitions are Markov. Extending this to arbitrary partitions is a matter for future work.

Int. J. Bifurcation Chaos 1995.05:1181-1192. Downloaded from www.worldscientific.com
by THE UNIVERSITY OF NEW SOUTH WALES on 06/14/17. For personal use only.

References

Diamond, P., Kloeden, P. & Pokrovskii, A. "Analysis of an algorithm for computing invariant measures," To appear in *Nonlinear Analysis.*

Froyland, G. (Unpublished).

Khas'minskii, R. Z. [1963] "Principle of averaging for parabolic and elliptic differential equations and for Markov processes with small diffusion," *Theory of Probability and its Applications* **8**(1), 1–21.

Kifer, Y. [1988] *Random Perturbations of Dynamical Systems, vol. 16 of Progress in Probability and Statistics* (Birkhauser, Boston).

Kohda, T. & Shinji, R. [1992] "A simple algorithm to approximate asymptotic measure on chaotic attractor of Hénon map," in *Proceedings of the 1992 Symposium on Nonlinear Theory and its Applications, Kanagawa, July 1992*, pp. 99–102.

Mees, A. I. [1991] "Dynamical systems and tesselations: Detecting determinism in data," *Int. J. of Bifurcation and Chaos* **1**(4), 777–794.

Mees, A. I., Murao, K., Judd, K. & Froyland, G. [1993] "Triangulations on tori and density estimation," in *Proceedings of the 1993 International Symposium on Nonlinear Theory and its Applications, Hawaii, December 1993*, vol. 1, pp. 275–280.

Ruelle, D. [1976] "A measure associated with axiom-A attractors," *Am. J. of Math.* **98**(3), 619–654.

Sauer, T., Yorke, J. A. & Casdagli, M. [1991] "Embedology," *J. of Stat. Phys.* **65**(3–4), 579–616.

Watson, D. F. [1981] "Computing the n-dimensional Delaunay tessellation with application to Voroni polytopes," *The Computer Journal* **24**(2), 167–172.

Watson. D. F. [1992] *Contouring: A Guide to the Analysis and Display of Spatial Data* (Pergamon Press).

Young. L.-S. [1986] "Stochastic stability of hyperbolic attractors," *Ergodic Theory and Dynamical Systems* **6**, 311–319.